Available online at www.sciencedirect.com
ScienceDirect
Trans. Nonferrous Met. Soc. China 32(2022) 1010−1018
Transactions of Nonferrous Metals Society of China
www.tnmsc.cn

Effect of sodium carbonate addition on carbothermic reduction of ilmenite concentrate

Xiao-dong LÜ[1], Dan CHEN[1], Yun-tao XIN[1,2], Wei LÜ[1], Xue-wei LÜ[1,2]

1. College of Materials Science and Engineering, Chongqing University, Chongqing 400044, China;
2. Chongqing Key Laboratory of Vanadium−Titanium Metallurgy and Advanced Materials, Chongqing University, Chongqing 400044, China

Received 2 March 2021; accepted 26 October 2021

Abstract: The enhanced reduction mechanism and kinetics of different Na_2CO_3 additions in the carbothermic reduction of ilmenite concentrate were investigated. The reduction process was carried out at different heating rates in a thermogravimetry facility, and the kinetics was studied using the Starink method. The results indicate that Na_2CO_3 addition enhanced the reduction effect as well as reduced the initial temperature of the reaction and the activation energy by increasing reactant activity in reactant form; however, it deteriorated the late-stage kinetic conditions by generating a molten phase, thereby reducing the reaction rate in the late stages of reduction. The average apparent activation energies of ilmenite concentrate with 0%, 3%, and 6% Na_2CO_3 are 447, 289, and 430 kJ/mol, respectively. The results from kinetics parameters confirm that Na_2CO_3 addition accelerated the reduction kinetics; however, excessive addition worsened the reduction kinetics.

Key words: ilmenite concentrate; non-isothermal kinetics; reduction mechanism; apparent activation energy

1 Introduction

Titanium dioxide is the most widely used white pigment, and 90% of titanium-bearing raw materials are used to produce titanium dioxide [1]. Furthermore, the chloride process has become the main and most advanced process in the titanium dioxide industry owing to its simplicity, low environmental pollution, and good product quality, accounting for 68% of the titanium dioxide production capacity. However, the high-titanium slag requirement for the chloride process is significant [2,3]. Currently, electric furnace smelting is the dominant technology for producing high-titanium slag from ilmenite concentrate. However, high-grade titanium reserves are gradually depleting due to the rapid development of the titanium industry worldwide. The energy consumption of electric arc furnaces may be high when low-grade ilmenite concentrate resources are used [4]; therefore, a novel and low energy-consuming process is required to produce titanium slag from low-grade ilmenite concentrate for the chloride process.

The key procedure in preparing titanium slag is the separation of slag from iron in reduced-ilmenite concentrate. In recent years, studies regarding ilmenite concentrate have been primarily focused on the reduction process [5−7]. In addition, most studies were focused on improving the reduction using additives [8,9], pre-oxidation treatment [10−12], mechanical activation [13−15], and other treatment methods [16,17], as shown in Table 1. HUANG et al [18] studied vacuum carbothermic reduction of Panzhihua ilmenite

Corresponding author: Xue-wei LÜ, Tel: +86-13658335559, E-mail: lvxuewei@163.com;
Yun-tao XIN, Tel: +86-18580090137, E-mail: xinyuntao0707@163.com
DOI: 10.1016/S1003-6326(22)65850-3
1003-6326/© 2022 The Nonferrous Metals Society of China. Published by Elsevier Ltd & Science Press

Table 1 Comparison of different enhancement methods for ilmenite concentrate reduction

Method	Action mechanism
Pre-oxidation	Destruct mineral structure; form new phase; form pores; increase specific surface area
Additive	Increase lattice distortion energy; promote atomic transport; provide reaction heat
Mechanical activation	Increase reaction activity and surface free energy

concentrate, which can effectively remove impurities such as calcium and magnesium to obtain a high-grade titanium. YU et al [19] investigated a clean and efficient route for ilmenite concentrate utilization through direct carbothermic reduction by adding high Na_2CO_3 dosages in a microwave field. LV et al [20] reported an economical and clean method for semi-molten reduction followed by magnetic separation to produce titanium slag from ilmenite concentrate. Additives can promote the growth of metal particles, thereby providing a basis for the subsequent separation of slag iron. Therefore, a novel and low energy-consuming semi-molten reduction process is proposed to effectively utilize ilmenite concentrate and reduce energy consumption. In this process, the reduction condition is enhanced with Na_2CO_3 addition to produce high-quality titanium slag. However, the enhanced reduction mechanism and kinetics of different Na_2CO_3 additions on the carbothermic reduction of ilmenite concentrate need to be further studied in the semi-molten reduction process.

The aim of this study is to elucidate the effect of Na_2CO_3 addition on the carbothermic reduction of ilmenite concentrate, both thermodynamically and kinetically, based on the activation energies, gas product analysis, reaction mechanism, and phase composition. These factors were compared systematically using the thermogravimetric (TG)−mass spectrometry method, which is useful for the selection of the semi-molten reduction process parameters.

2 Experimental

The ilmenite concentrate used in the experiment is the concentrate obtained via the ilmenite ore beneficiation process. The chemical composition and X-ray diffraction pattern of the ilmenite concentrate used in the experiment, as shown in Table 2 and Fig. 1, respectively, indicate that the main phases in the ilmenite concentrate were $FeTiO_3$ and Fe_2O_3. Most of the ilmenite concentrate particles were measured to be 48−150 μm. The reducing agent was graphite powder with ≥99.9% in purity and a particle size of <13 μm.

Table 2 Chemical composition of ilmenite concentrates as pure oxides (wt.%)

TiO_2	FeO	Fe_2O_3	SiO_2	MnO	MgO	CaO	V_2O_5	Al_2O_3
45.73	32.41	17.09	2.68	0.78	0.59	0.26	0.198	0.163

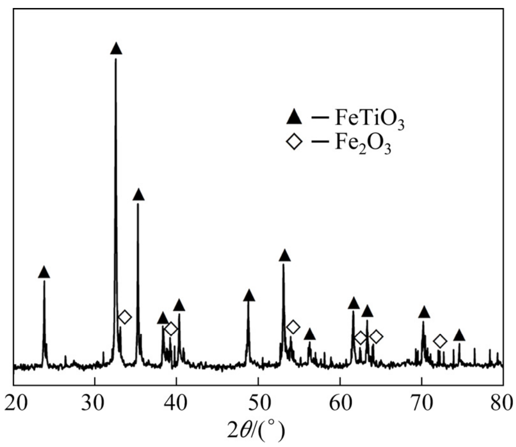

Fig. 1 XRD pattern of ilmenite concentrate used in this study

A Setaram Evo TG−DTA 1750 thermal analyzer was used to conduct the TG experiments. Based on previous studies, 0, 3, and 6 wt.% Na_2CO_3 were added to ilmenite concentrate and graphite in the reduction experiment, and the dosage of the reducer was set to be 13 wt.% [21,22]; at this concentration, the semi-molten reduction of ilmenite concentrate can yield significant results. The maximum temperature of the non-isothermal process was 1673 K, and the heating rates (β) adopted in the experiments were 10, 15, and 20 K/min. The sample ((30±0.9) mg) was placed in an alumina crucible with a height of 8 mm and diameter of 6 mm. The reaction vessel was pumped first, and then Ar (99.999%) was charged in the reaction vessel at a flow rate of 20 mL/min. The operating pressure was 1.013×10^5 Pa, and the reduction process from low to high temperature was carried out at different heating rates in the thermogravimetry facility. The content of tail gas generated from the chemical reaction was detected in real time using a TILON LC−D200 mass spectroscopy system. The reduction degree was obtained from the thermal mass curve, and the tail gas analysis data and the kinetics were studied using the Starink method.

3 Results and discussion

3.1 TG/DTG analysis

The TG/DTG results and the relative content of the CO/CO_2 curves for the carbothermic reduction of ilmenite concentrate with different amounts of Na_2CO_3 at various heating rates (10, 15, and 20 K/min) are shown in Fig. 2.

As shown in Fig. 2, the trend of the TG/DTG curves was similar at different heating rates. However, the starting temperature of reduction increased gradually as the heating rate increased because heat lag occurred during heating. The higher the heating rate was, the more significant the heat lag was. Meanwhile, the DTG curves show that the temperature increased gradually at the maximum reduction as the heating rate increased.

As shown by the relative volume fraction changes of CO and CO_2, the relative volume fraction of CO_2 increased significantly in the corresponding temperature range (<1120 K). Moreover, with an increase in the Na_2CO_3 content, the DTG peak intensity of the corresponding region increased, and the relative volume fraction of CO_2 extended to the low-temperature region, indicating that the thermal decomposition temperature range of Na_2CO_3 and the decomposition rate increased. With an increase in temperature, the DTG curves dropped rapidly, the relative volume fraction of CO increased rapidly after approximately 1150 K, and a large number of reduction reactions began. The reduction reaction and the gasification reaction of carbon began in this stage, resulting in a significant amount of CO formation. Compared with the addition of 0% Na_2CO_3 (approximately 1300 K), the temperature decreased by approximately 150 K.

3.2 Reduction degree analysis

A reduction experiment was performed at 1673 K. At this temperature, titanium oxide was reduced to Ti_3O_5, and iron oxide was reduced to metal iron [21]. The mass loss of ilmenite concentrate was primarily caused by the formation of CO and CO_2 during reduction process. Therefore,

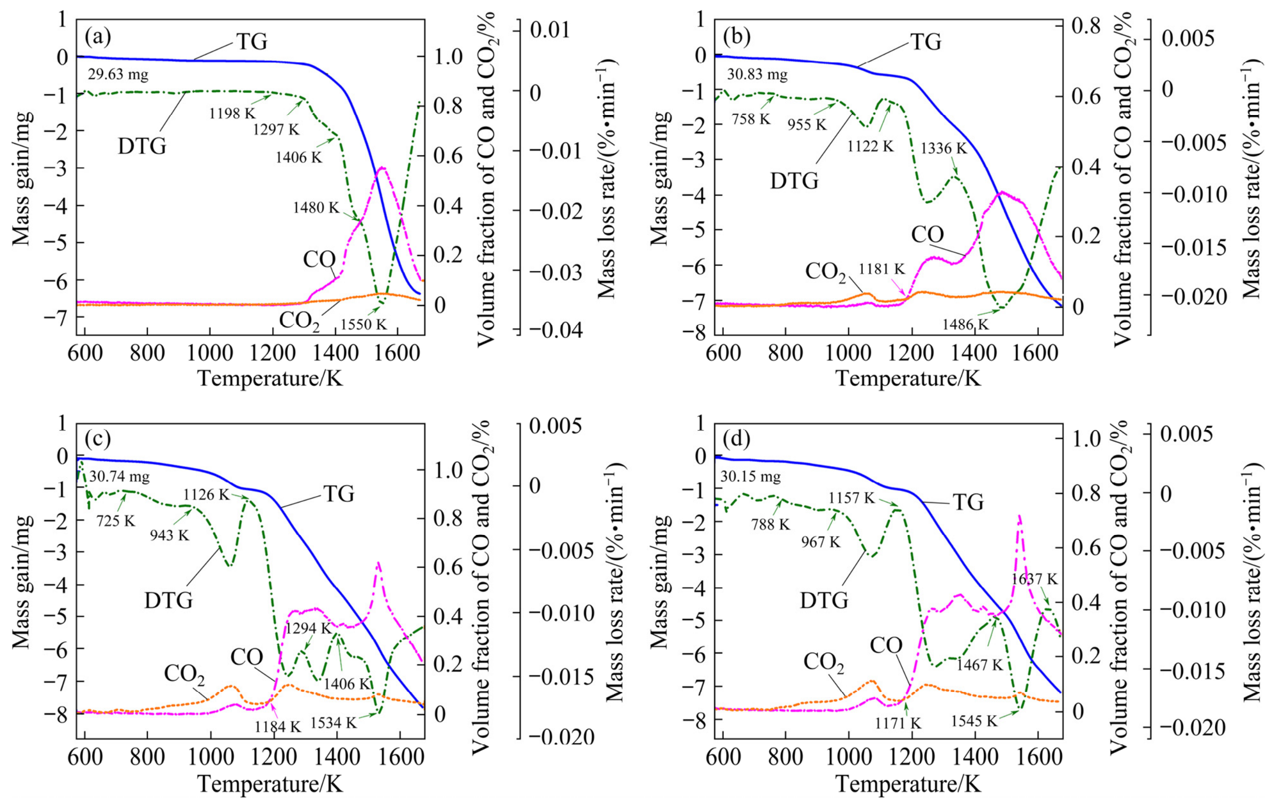

Fig. 2 TG/DTG curves of solid-state reduction of ilmenite concentrate under different conditions: (a) No Na_2CO_3 addition, heating rate of 10 K/min; (b) 3% Na_2CO_3 addition, heating rate of 10 K/min; (c) 6% Na_2CO_3 addition, heating rate of 10 K/min; (d) 6% Na_2CO_3 addition, heating rate of 20 K/min

the reduction degree of the sample during the reduction process was calculated based on oxygen loss.

As mentioned above, the CO_2 produced via Na_2CO_3 decomposition [23,24] caused the change in TG/DTG curves prior to approximately 1100 K, whereas the reaction of ilmenite concentrate began at approximately 1120 K. Meanwhile, the Na_2O produced via the decomposition reacted with the ilmenite concentrate to form sodium−titanium oxide with a low melting temperature [21,25], which provided the kinetic conditions [21] for the subsequent reduction of ilmenite concentrate, resulting in a favorable effect. Therefore, the calculation of ilmenite concentrate reduction degree should exclude the mass change caused by Na_2CO_3 decomposition.

The theoretical oxygen loss is calculated as follows:

$$m_{\Sigma O_{(theory)}}=\left(\frac{1}{6}m_{O_{(TiO_2)}}+m_{O_{(FeO)}}+m_{O_{(Fe_2O_3)}}\right)\times m_{(ilmenite)}=(\frac{1}{6}\times 0.4573\times\frac{32}{79.87}+0.3241\times\frac{16}{71.85}+0.1709\times\frac{48}{159.69})\times m_{(ilmenite)}=0.1541m_{(ilmenite)} \quad (1)$$

The actual oxygen loss is calculated as follows:

$$m_{\Sigma O_{(reality)}}=\Delta m_{\Sigma O}-m_{\Sigma O_{(Na_2CO_3)}}=\Delta m_{O_{(CO)}}+\Delta m_{O_{(CO_2)}}+m_{\Sigma O_{(Na_2CO_3)}}=\frac{16}{28}\times\Delta m_{ilmenite}\times\frac{\varphi(CO)}{\varphi(CO)+\varphi(CO_2)}+\frac{32}{44}\times\Delta m_{ilmenite}\times\frac{\varphi(CO_2)}{\varphi(CO)+\varphi(CO_2)}-m_{\Sigma O_{(Na_2CO_3)}} \quad (2)$$

Therefore, the reduction degree (α) of the sample is defined as

$$\alpha=\frac{m_{\Sigma O_{(reality)}}}{m_{\Sigma O_{(theory)}}} \quad (3)$$

where $m_{\Sigma O_{(theory)}}$ is the total theoretical mass of the O atom; $m_{O_{(TiO_2)}}$, $m_{O_{(FeO)}}$, and $m_{O_{(Fe_2O_3)}}$ are the O atom masses of TiO_2, FeO, and Fe_2O_3 in the sample, respectively; $m_{(ilmenite)}$ is the mass of ilmenite concentrate in the experiment; $m_{\Sigma O_{(reality)}}$ is the actual mass loss of O atoms; $\Delta m_{\Sigma O}$ is the mass loss of the O atoms; $m_{\Sigma O_{(Na_2CO_3)}}$ is the mass loss of O atoms in Na_2CO_3; $\Delta m_{O_{(CO)}}$ is the O atom mass loss by CO; $\Delta m_{O_{(CO_2)}}$ is the O atom mass loss due to CO_2. Additionally, $\varphi(CO)+\varphi(CO_2)=100\%$, where φ is the mass fraction of the species in the gas (because the gas analysis varies with temperature, the φ values are integrated values over time). Finally, $\Delta m_{ilmenite}$ is the mass loss of the sample.

The reduction degree of ilmenite concentrate under different conditions is shown in Fig. 3. As shown, the reduction time of the sample at the same temperature decreased with an increase in heating rate, thereby resulting in a decrease in the reduction degree of the sample. In addition, the reaction could be performed in advance, which improved the maximum reduction degree of the sample with Na_2CO_3 addition. Meanwhile, the effect of heating rate on the reduction degree became less prominent as the Na_2CO_3 content increased. However, the reaction rate was affected, although Na_2CO_3 addition promoted the advancement of the reaction. The reduction degree (α) and time (t) at a heating rate of 10 K/min were integrated to investigate the relationship between the reaction rates more effectively [26], as shown in Fig. 4.

As shown in Fig.4, the reduction rate increased with the amount of Na_2CO_3 in the low-temperature region because Na_2CO_3 caused the reaction to occur in advance by participating in the reaction. However, as the temperature increased, the reduction rates without Na_2CO_3 increased rapidly

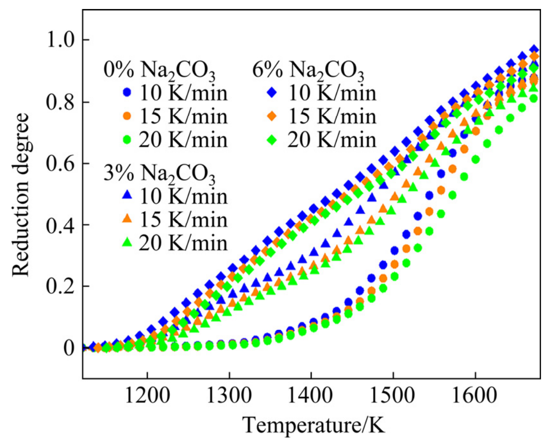

Fig. 3 Reduction degree of ilmenite concentrate under different conditions

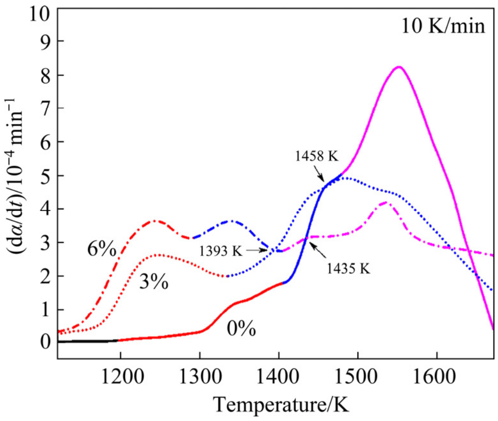

Fig. 4 First derivatives of conversion degree (α) versus time (t) for different amounts of Na_2CO_3

and were higher than those of 3% and 6% Na_2CO_3 at 1435 and 1458 K, respectively. In addition, the reaction rate of the 3% Na_2CO_3 sample exceeded that of the 6% Na_2CO_3 sample at 1393 K, indicating that Na_2CO_3 addition caused the reduction reaction to occur in advance; however, this caused the reaction rate to decrease in the high-temperature stage. This occurred because Na_2CO_3 caused the sample to generate a molten phase with a low melting point [21,25], which was not conducive to gas diffusion and hence deteriorated the kinetic conditions; consequently, the reaction rate decreased.

As shown in Fig. 4, for the case without Na_2CO_3, the chemical reactions were categorized into three stages based on the peak curves, i.e., 1198−1406 K (0−0.09), 1406−1480 K (0.09−0.25), and 1480−1673 K (0.25−0.88). For the case with 3% Na_2CO_3, the chemical reactions were categorized into two stages based on the peak curves, i.e., 1122−1336 K (0−0.21) and 1336−1673 K (0.21−0.92). Finally, for the case with 6% Na_2CO_3, the chemical reactions were categorized into three stages based on the peak curves, i.e., 1126−1294 K (0−0.24), 1294−1406 K (0.24−0.45), and 1406−1673 K (0.45−0.97). As mentioned above, Na_2CO_3 addition is more conducive to the reaction of the first stage, but an excessive addition worsens the reaction rate of the second and third stages. Therefore, the addition of 3% Na_2CO_3 was optimal for reduction.

3.3 Reduction process analysis

The primary chemical reactions for the enhanced carbothermic reduction of ilmenite concentrate were categorized into four parts, namely, decomposition reaction, Boudouard reaction, solid−solid interaction, and gas−solid interaction. The primary reactions are given in Table 3, and the relationship between the Gibbs free energy change and temperature is shown in Fig. 5. In addition, the primary chemical reactions at different stages with different Na_2CO_3 amounts can be categorized by analyzing Fig. 4 and Table 3, as shown in Fig. 6.

Table 3 Primary reactions in reduction

Type	Equation	Relation between Δ_rG^0 and T	
Decomposition reaction	$Na_2CO_3=Na_2O+CO_2$	$\Delta_rG^0=296.89-0.119T$	(4)
Boudouard reaction	$CO_2+C=2CO$	$\Delta_rG^0=168.53-0.173T$	(5)
Solid−solid interaction	$3Fe_2O_3+C=2Fe_3O_4+CO$	$\Delta_rG^0=130.44-0.222T$	(6)
	$Fe_3O_4+C=3FeO+CO$	$\Delta_rG^0=188.40-0.197T$	(7)
	$FeO+C=Fe+CO$	$\Delta_rG^0=150.18-0.151T$	(8)
	$FeTiO_3+C=Fe+TiO_2+CO$	$\Delta_rG^0=173.86-0.154T$	(9)
	$FeTiO_3+Na_2O+C=Fe+Na_2TiO_3+CO$	$\Delta_rG^0=-64.93-0.139T$	(10)
	$3TiO_2+C=Ti_3O_5+CO$	$\Delta_rG^0=257.55-0.170T$	(11)
Gas−solid interaction	$3Fe_2O_3+CO=2Fe_3O_4+CO_2$	$\Delta_rG^0=-38.09-0.049T$	(12)
	$Fe_3O_4+CO=3FeO+CO_2$	$\Delta_rG^0=19.87-0.024T$	(13)
	$FeO+CO=Fe+CO_2$	$\Delta_rG^0=-18.36+0.022T$	(14)
	$FeTiO_3+CO=Fe+TiO_2+CO_2$	$\Delta_rG^0=5.32+0.018T$	(15)
	$FeTiO_3+Na_2O+CO=Fe+Na_2TiO_3+CO_2$	$\Delta_rG^0=-233.46+0.034T$	(16)
	$3TiO_2+CO=Ti_3O_5+CO_2$	$\Delta_rG^0=89.02+0.002T$	(17)

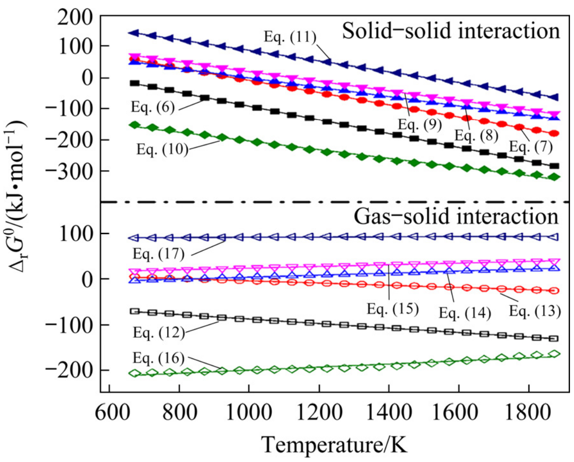

Fig. 5 Relationship between Gibbs free energy and temperature

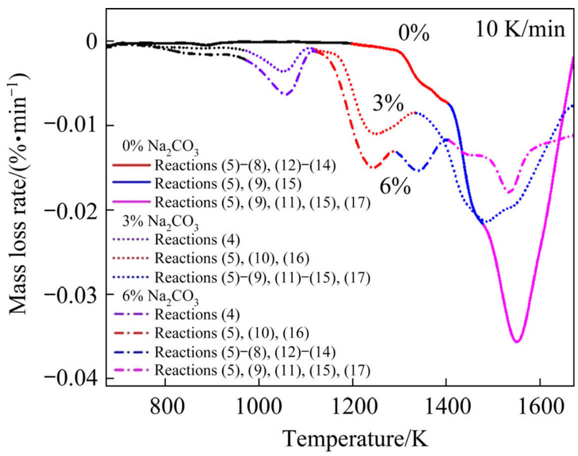

Fig. 6 Primary chemical reactions at different stages with different Na_2CO_3 amounts

Figure 6 shows that Na_2CO_3 addition accelerated the reaction, but the mass loss rate of the sample was lower than that of the sample without Na_2CO_3 as the temperature increased, i.e., the reaction rate decreased. In addition, the changing trend in Fig. 6 was similar to that in Fig. 4; therefore, the segmented reaction stages were similar. The reaction sequence of the ilmenite concentrate without Na_2CO_3 was as follows: the reduction of iron oxides (Eqs. (6)−(8) and (12)−(14)), followed by those of ilmenite concentrate (Eqs. (9) and (15)) and titanium oxide (Eqs. (11) and (17)). However, when the Na_2CO_3 amount was increased, Na_2CO_3 decomposition occurred at a temperature lower than 1120 K (Eq. (4)), and Na_2O produced by Na_2CO_3 decomposition participated in the reaction of ilmenite concentrate, reducing the initial temperature of the reaction. Therefore, the chemical reactions (Eqs. (10) and (16)) occurred first, and then the reaction was carried out in the normal order.

During the reduction process, the gasification reaction of carbon (Boudouard reaction [27]) always occurred, and the CO produced by the reaction participated in the gaseous reductions (Eqs. (12)−(17)). However, the gaseous reduction (Eqs. (12)−(17)) had small reaction equilibrium constants and the reduction occurred in an open furnace; therefore, only the solid material near the bottom layer proceeded through gaseous reduction (Eqs. (12)−(17)). As shown in Fig. 2, the relative volume fraction of CO_2 was extremely low when the temperature exceeded 1120 K.

3.4 Reaction activation energy

Based on the non-isothermal kinetic theory, the reaction activation energy can be calculated via the Starink method [28]. The Starink equation is expressed as

$$\ln\left(\frac{\beta}{T^{1.92}}\right)=C-1.0008\frac{E}{RT} \tag{18}$$

where β is the heating rate, T is the thermodynamic temperature corresponding to the degree of conversion (α) in the experiment with heating rate β, E is the apparent activation energy, and R is the gas constant.

The fitting of the relationship of $\ln(\beta/T^{1.92})$ to $-1.0008/T$ via the conversion method and the apparent activation energy corresponding to different conversion rates are shown in Fig. 7. The average apparent activation energies of the ilmenite concentrate with 0%, 3%, and 6% Na_2CO_3 were 447, 289, and 430 kJ/mol, respectively.

To reveal the change mechanism of the apparent activation energy, the relationship between activation energy and temperature was described in a simple manner, as shown in Fig. 8. Figure 8 shows that the reactant activity was low owing to the low reduction temperature in the early stage of the reaction. Therefore, the chemical reaction governed the reduction process and resulted in a higher activation energy at that stage. However, the energy of the activated molecules increased with temperature, making it easier to transcend the reaction barrier for the chemical reaction. Therefore, the limitation of the chemical reaction during the reduction process weakened steadily, and the diffusion of the reactant gradually became the limiting step of reduction process. Consequently,

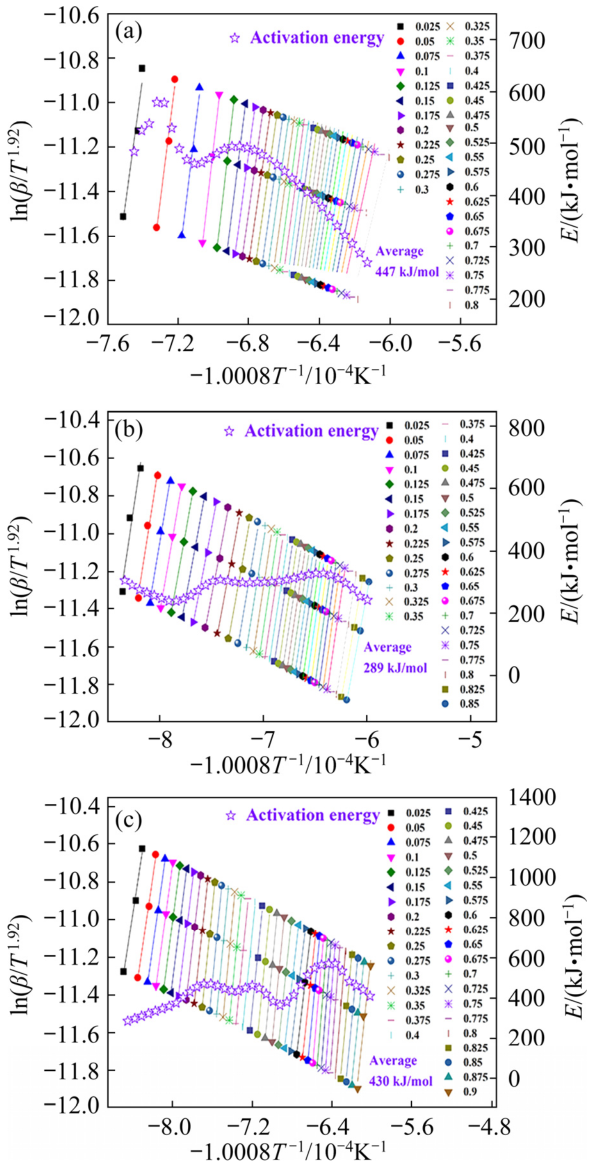

Fig. 7 $\ln(\beta/T^{1.92})$−(−1.0008/T) curves at different α values and apparent activation energy: (a) 0% Na_2CO_3; (b) 3% Na_2CO_3; (c) 6% Na_2CO_3

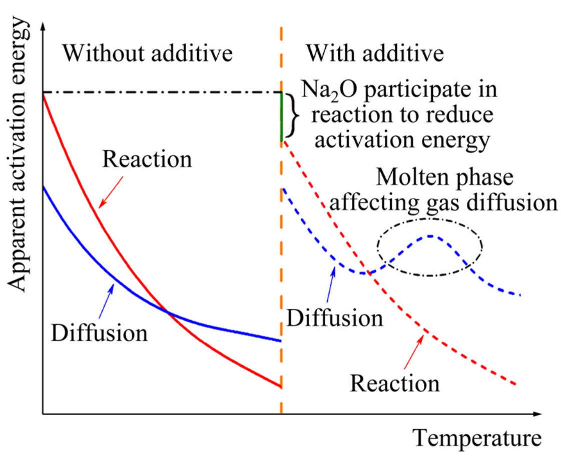

Fig. 8 Relationship between apparent activation energy and temperature

the apparent activation energy decreased gradually.

However, when the Na_2CO_3 was added, as mentioned above, Na_2CO_3 decomposed into Na_2O and CO_2 on heating [21,25]. Unlike the catalyst, Na_2O exhibited high activity and participated in the ilmenite concentrate reduction process, thereby increasing reactant activity in reactant form and reducing the initial temperature of the reaction and the activation energy. Meanwhile, the addition of alkali metal oxides catalyzed the gasification of carbon, thereby promoting the reaction [29,30]. Therefore, the apparent activation energy with Na_2CO_3 was lower than that without Na_2CO_3 in the early stages of the reaction. However, Na_2O reacted with ilmenite concentrate (Eqs. (10) and (16)) to form sodium titanates with a low melting point and gradually formed a molten phase as the temperature increased. The molten phase was not conducive to gas diffusion; in fact, it deteriorated the kinetic conditions and resulted in an increase in the activation energy. The molten phase increased as the Na_2CO_3 content increased to 6%, thereby resulting in an increase in the activation energy that exceeded that for the case without additives.

Nevertheless, the molten phase formed at a high temperature was beneficial to accelerating mass transfer [31]. This prevented the formation of wrapped metal shells by metal iron formed during the reduction process [32] and promoted the nucleation growth of the metallic iron, thereby facilitating the subsequent separation of metal from the slag.

4 Conclusions

(1) The trend of the reaction degree curves with the same raw material was similar under different heating rates. The starting reduction temperature and the temperature at the maximum reduction rate increased gradually as the heating rate increased. Compared to the case without Na_2CO_3, the starting reduction temperature of the case with Na_2CO_3 was decreased by approximately 150 K.

(2) Na_2O exhibited high activity and participated in the ilmenite concentrate reduction process, thereby increasing reactant activity in reactant form and reducing the initial temperature of the reaction and the activation energy. However, it deteriorated the kinetic conditions by generating a

liquid phase, thereby reducing the reaction rate and leading to an increase in the apparent activation energy.

(3) As the temperature increased, the governing factor for the reduction of ilmenite concentrate gradually changed from chemical reactions to diffusion. For cases with 0%, 3%, and 6% Na_2CO_3, the average apparent activation energies of ilmenite concentrate were 447, 289, and 430 kJ/mol, respectively.

Acknowledgments

This work was supported by the National Natural Science Foundation of China (No. U1902217).

References

[1] HAN Yan-fang, SUN Ti-chang, LI Jie, QI Tao, WANG Li-na, QU Jing-kui. Preparation of titanium dioxide from titania-rich slag by molten NaOH method [J]. International Journal of Minerals Metallurgy and Materials, 2012, 19(3): 205−211.

[2] WAN He-li, XU Bao-qiang, DAI Yong-nian, YANG Bin, LIU Da-chun, SEN Wei. Preparation of titanium powders by calciothermic reduction of titanium dioxide [J]. Journal of Central South University, 2012, 19(9): 2434−2439.

[3] KANG J, MOON G, KIM M S, OKABE T H. Production of high-grade titanium dioxide directly from titanium ore using titanium scrap and iron chloride waste [J]. Metals and Materials International, 2019, 25(1): 257−267.

[4] HUANG Run, LV Xue-wei, BAI Chen-guang, DENG Qin-yu, MA S. Solid state and smelting reduction of Panzhihua ilmenite concentrate with coke [J]. Canadian Metallurgical Quarterly, 2012, 51(4): 434−439.

[5] GOU Hai-peng, ZHANG Guo-hua, YUAN Xin, CHOU Kuo-chih. Formation of titanium carbonitride via carbothermic reduction of ilmenite concentrate in nitrogen atmosphere [J]. ISIJ International, 2016, 56(5): 744−751.

[6] LV Xiao-dong, HUANG Run, WU Qin-zhi, XU Ben-jun, ZHANG Jin-zhu. Non-isothermal reduction kinetics during vacuum carbothermal reduction of ilmenite concentrate [J]. Vacuum, 2019, 160: 139−145.

[7] GOU Hai-peng, ZHANG Guo-hua, HU Xiao-jun, CHOU Kuo-chih. Kinetic study on carbothermic reduction of ilmenite with activated carbon [J]. Transactions of Nonferrous Metals Society of China, 2017, 27(8): 1856−1861.

[8] GENG Chao, SUN Ti-chang, YANG Hui-fen, MA You-wen, GAO En-xia, XU Cheng-yan. Effect of Na_2SO_4 on the embedding direct reduction of beach titanomagnetite and the separation of titanium and iron by magnetic separation [J]. ISIJ International, 2015, 55(12): 2543−2549.

[9] SONG Bing, LV Xue-wei, MIAO Hubet Hui-jun, HAN Ke-xi, ZHANG Kai, HUANG Run. Effect of $Na_2B_4O_7$ addition on carbothermic reduction of ilmenite concentrate [J]. ISIJ International, 2016, 56(12): 2140−2146.

[10] CHEN De-sheng, SONG Bo, WANG Li-na, QI Tao, WANG Yong, WANG Wei-jing. Solid state reduction of Panzhihua titanomagnetite concentrates with pulverized coal [J]. Minerals Engineering, 2011, 24(8): 864−869.

[11] LV Wei, LV Xue-wei, XIANG Jun-yi, ZHANG Ying-yi, LI Sheng-ping, BAI Chen-guang, SONG Bing, HAN Ke-xi. A novel process to prepare high-titanium slag by carbothermic reduction of pre-oxidized ilmenite concentrate with the addition of Na_2SO_4 [J]. International Journal of Mineral Processing, 2017, 167: 68−78.

[12] GOU Hai-peng, ZHANG Guo-hua, CHOU Kuo-chih. Influence of pre-oxidation on carbothermic reduction process of ilmenite concentrate [J]. ISIJ International, 2015, 55(5): 928−933.

[13] BOGATYREVA E V, CHUB A V, ERMILOV A G. Forecasting preliminary mechanical activation effect on arizonite and ilmenite concentrates by X-ray crystal analysis [J]. Journal of Mining Science, 2014, 50(2): 385−398.

[14] LI Chun, LIANG Bin, GUO Ling-hong, WU Zi-bin. Effect of mechanical activation on the dissolution of Panzhihua ilmenite [J]. Minerals Engineering, 2006, 19(14): 1430−1438.

[15] ZHANG Li, HU Hui-ping, WEI Liang-ping, CHEN Qi-yuan, TAN Jun. Effects of mechanical activation on the hcl leaching behavior of titanaugite, ilmenite, and their mixtures [J]. Metallurgical and Materials Transactions B−Process Metallurgy and Materials Processing Science, 2010, 41(6): 1158−1165.

[16] SALMANI NURI Omid, IRANNAJAD Mehdi, MEHDILO Akbar. Effect of surface dissolution on kinetic parameters in flotation of ilmenite from different gangue minerals [J]. Transactions of Nonferrous Metals Society of China, 2019, 29(12): 2615−2626.

[17] LU Chang-yuan, ZOU Xing-li, LU Xiong-gang, XIE Xue-liang, ZHENG Kai, XIAO Wei, CHENG Hong-wei, LI Guang-shi. Reductive kinetics of Panzhihua ilmenite with hydrogen [J]. Transactions of Nonferrous Metals Society of China, 2016, 26(12): 3266−3273.

[18] HUANG Run, LIU Peng-sheng, QIAN Xing, ZHANG Jin-zhu. Comprehensive utilization of Panzhihua ilmenite concentrate by vacuum carbothermic reduction [J]. Vacuum, 2016, 134: 20−24.

[19] YU Zhi-gang, XIAO Jing-wu, LENG Hai-yan, CHOU Kuo-chih. Direct carbothermic reduction of ilmenite concentrates by adding high dosage of Na_2CO_3 in microwave field [J]. Transactions of Nonferrous Metals Society of China, 2021, 31(6): 1818−1827.

[20] LV Wei, BAI Chen-guang, LV Xue-wei, HU Kai, LV Xue-ming, XIANG Jun-yi, SONG Bing. Carbothermic reduction of ilmenite concentrate in semi-molten state by adding sodium sulfate [J]. Powder Technology, 2018, 340: 354−361.

[21] LV Xiao-dong, XIN Yun-tao, LV Xue-wei, LV Wei, DANG Jie. High-titanium slag preparation process by carbothermic reduction of ilmenite and wet-magnetic separation [J]. Metallurgical and Materials Transactions B, 2020, 52(1): 351−362.

[22] LV Wei, ELLIOTT R, LV Xue-wei, XIANG Jun-yi, WANG Fan-mao, YANG Yin-dong, BARATI M. Generation of titania-rich slag and iron from ilmenite concentrate by carbothermic reduction and magnetic separation in the presence of Na_2CO_3 [J]. Canadian Metallurgical Quarterly, 2020, 59(4): 393−404.

[23] PERÍGOLO D M, DE PAULA F G F, ROSMANINHO M G, DE SOUZA P P, LAGO R M, ARAUJO M H. Conversion of fatty acids into hydrocarbon fuels based on a sodium carboxylate intermediate [J]. Catalysis Today, 2017, 279: 260−266.

[24] YAN Ke-zhou, GUO Yan-xia, LIU Dan-dan, MA Zhi-bin, CHENG Fang-qin. Thermal decomposition and transformation mechanism of mullite with the action of sodium carbonate [J]. Journal of Solid State Chemistry, 2018, 265: 326−331.

[25] ELTAWIL S Z, MORSI I M, YEHIA A, FRANCIS A A. Alkali reductive roasting of ilmenite ore [J]. Canadian Metallurgical Quarterly, 1996, 35(1): 31−37.

[26] LV Wei, LV Xue-ming, LV Xue-wei, XIANG Jun-yi, BAI Chen-guang, SONG Bing. Non-isothermal kinetic studies on the carbothermic reduction of Panzhihua ilmenite concentrate [J]. Mineral Processing and Extractive Metallurgy−Transactions of the Institutions of Mining and Metallurgy, 2019, 128(4): 239−247.

[27] ELGUINDY M I, DAVENPORT W G. Kinetics and mechanism of ilmenite reduction with graphite [J]. Metallurgical and Materials Transactions B, 1970, 1(6): 1729−1734.

[28] STARINK M J. The determination of activation energy from linear heating rate experiments: a comparison of the accuracy of isoconversion methods [J]. Thermochimica Acta, 2003, 404(1/2): 163−176.

[29] MCKEE D M. Mechanisms of the alkali metal catalysed gasification of carbon [J]. Fuel, 1983, 62: 170−175.

[30] WOOD B J, FLEMING R H, WISE H. WISE Henry. Reactive intermediate in the alkali-carbonate-catalysed gasification of coal char [J]. Fuel, 1984, 63: 1600−1603.

[31] DIAO Jiang, LIU Xuan, ZHANG Tao, XIE Bing. Mass transfer of phosphorus in high-phosphorus hot-metal refining [J]. International Journal of Minerals Metallurgy and Materials, 2015, 22(3): 249−253.

[32] LI Wen-bing, YUAN Zhang-fu, XU Cong, PAN Yi-fang, WANG Xiao-qiang. Effect of temperature on carbothermic reduction of ilmenite [J]. Journal of Iron and Steel Research International, 2005, 12(4): 1−5.

添加剂 Na_2CO_3 对钛精矿碳热还原的影响

吕晓东[1]，陈 丹[1]，辛云涛[1,2]，吕 炜[1]，吕学伟[1,2]

1. 重庆大学 材料科学与工程学院，重庆 400044；
2. 重庆大学 钒钛冶金及新材料重庆市重点实验室，重庆 400044

摘 要：研究添加不同含量的 Na_2CO_3 对钛精矿强化还原机理和动力学的影响，以不同的升温速率进行还原过程，并采用 Starink 方法研究其动力学。结果表明：Na_2CO_3 的加入强化还原效果，并通过以反应物的形式增加其活性来降低还原反应的初始温度和表观活化能；然而，Na_2CO_3 的加入会形成熔融相恶化还原后期的动力学条件，从而降低还原后期的反应速率。当 Na_2CO_3 添加量分别为 0%、3% 和 6% 时，还原过程的平均表观活化能为 447、289 和 430 kJ/mol。动力学参数表明，添加 Na_2CO_3 能改善还原动力学条件，但添加过量会恶化还原动力学条件。

关键词：钛精矿；非等温动力学；还原机理；表观活化能

(Edited by Bing YANG)